

## Intermetallic Phases as Thermoelectrics

Christophe Candolfi, Jing-Tai Zhao<sup>1</sup>, Horst Borrmann, Michael Baitinger, Q.-G. Cao<sup>1</sup>, Raul Cardoso-Gil, H.-H. Chen<sup>1</sup>, K. Guo<sup>1</sup>, Z.-Y. Man<sup>1</sup>, Helge Rosner, Walter Schnelle, Maik Wagner, X.-J. Wang<sup>1</sup>, Hui Zhang<sup>1</sup>, Frank Steglich, and Yuri Grin

The last two decades have witnessed a renewed interest in power generation and refrigeration based upon thermoelectric (TE) effects. The design of highly efficient TE materials, however, requires an unusual combination of low electrical resistivity and thermal conductivity while, at the same time, achieving high thermopower [1a]. These three transport properties define the dimensionless figure of merit at a given temperature which controls the efficiency of a TE device. However, all these properties are interdependent making any attempt to improve the values a complex task. In an effort to overcome these difficulties and to push beyond the level of common compounds, several physical mechanisms were proposed to be employed, and strong experimental endeavors were taken to demonstrate a proof-of-principle [1a]. Among all the research directions explored in the last few years, two fruitful strategies resulted in the discovery of new efficient TE materials [1b]. A first one relies on the search for materials that exhibit complex crystal structures. Such structures may pave the way for minimizing the thermal conductivity while maintaining good electrical properties. These structures include skutterudites, clathrates and Zintl phases [2]. A second strategy is related to the search of semiconductors whose TE properties may be optimized through partial substitutions of the constituting elements. Here, we present examples which illustrate each one of these approaches: the Zintl phases displaying a 1:2:2 stoichiometry and the intermetallic compound  $\text{Ru}_{1-y}\text{In}_3$  and its ternary derivatives.

### The Zintl phases $AM_2\text{Sb}_2$

Over the last few years, in cooperation with our partner group, we have focused our attention on the synthesis, the crystal structure determination and the characterization of the transport properties of the Zintl phase compounds  $AM_2X_2$  (where  $A$  is an alkaline-earth or a divalent rare-earth metal,  $M$  is Zn or Cd, and  $X$  is typically Sb) with  $\text{CaAl}_2\text{Si}_2$

crystal structure type to assess their potential as thermoelectric materials [3–10]. Our goal is to improve the thermoelectric properties of the respective ternary Zintl compounds through substitutions on all the three crystallographic sites of the  $\text{CaAl}_2\text{Si}_2$ -type structure. By this means the chemical disorder can be enhanced and thus, the thermal conductivity reduced. We therefore investigated in detail the systems  $\text{Yb}_x\text{Eu}_{1-x}\text{Cd}_2\text{Sb}_2$ ,  $\text{Ca}_x\text{Yb}_{1-x}\text{Cd}_2\text{Sb}_2$ ,  $\text{YbZn}_x\text{Cd}_{2-x}\text{Sb}_2$ ,  $\text{Eu}(\text{Zn}_{1-x}\text{Cd}_x)_2\text{Sb}_2$  and  $\text{YbCd}_2\text{Sb}_{2-x}\text{Ge}_x$ .

All the samples investigated were prepared by reacting stoichiometric amounts of pure elements. The ingots obtained were ground and densified by spark plasma sintering. The thermoelectric properties were measured in the temperature range of 300 K – 800 K using a commercial set-up (ZEM-3 for measurement of  $\alpha$  and  $\rho$ , and laser flash technique for  $\kappa$ ). Significant improvement of the  $ZT$  values could be achieved through the different substitutions studied (Fig. 1).

The thermoelectric performance of  $\text{EuZn}_2\text{Sb}_2$  and  $\text{EuCd}_2\text{Sb}_2$  was optimized by mixed occupation of the transition-metal position. Samples of the solid solution  $\text{Eu}(\text{Zn}_{1-x}\text{Cd}_x)_2\text{Sb}_2$  were prepared from the elements for compositions with  $x = 0, 0.1, 0.3, 0.5$  and 1. The combination of low electrical resistivity, high thermopower and low lattice thermal conduc-

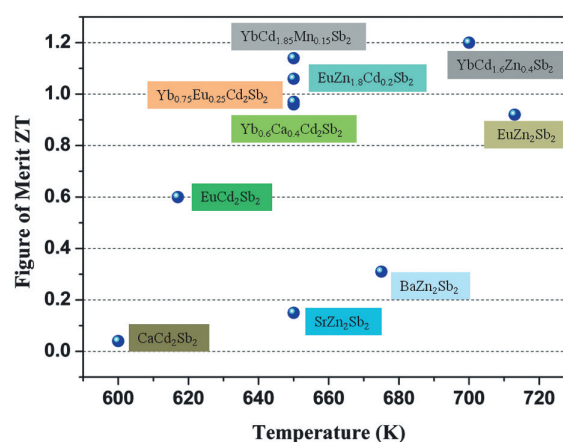


Fig. 1: Maximal thermoelectric figure of merit  $ZT$  in the 600 K – 720 K temperature range of the various ternary and quaternary systems investigated.

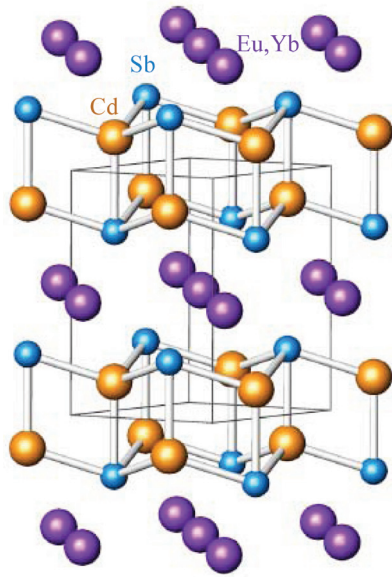


Fig. 2: Crystal structure of  $\text{Yb}_x\text{Eu}_{1-x}\text{Cd}_2\text{Sb}_2$  showing  $[\text{Cd}_2\text{Sb}_2]$  double layers and Eu and Yb cations between the layers.

tivity resulted in a comparatively high  $ZT$  value of 1.06 at 650 K for an optimum Cd content of  $x = 0.1$ .

Another way to improve the thermoelectric properties was realized upon substituting on the cationic site of the crystal structure of the  $\text{EuCd}_2\text{Sb}_2$  and  $\text{YbCd}_2\text{Sb}_2$  compounds. The thermoelectric properties of the solid solution  $\text{Yb}_x\text{Eu}_{1-x}\text{Cd}_2\text{Sb}_2$  were investigated for  $x = 0, 0.5, 0.75,$  and 1. The crystal structure (Fig. 2) is formed by double layers of corrugated hexagons of Cd and Sb, together with Eu and Yb between the layers. Upon substituting Yb by Eu, the lattice parameters were found to increase.

Figure 3 shows the thermoelectric properties of the four samples investigated within the temperature range 300 K – 650 K. These materials show rather low electrical resistivity values that vary between  $40 \text{ m}\Omega\text{cm}$  and  $90 \text{ m}\Omega\text{cm}$  at 650 K. Regardless of the Eu content, high thermopower values are achieved over the whole temperature range investigated. Owing to the complex crystal structure and chemical bonding of these compounds together with the enhanced disorder on the cationic site, low thermal conductivity values can be reached, similar to those encountered in clathrate compounds for instance. The combination of high thermopower values and low thermal conductivity results in maximum  $ZT$  values of 0.88 and 0.97 at 650 K for  $x = 0.5$  and  $x = 0.25$ , respectively.

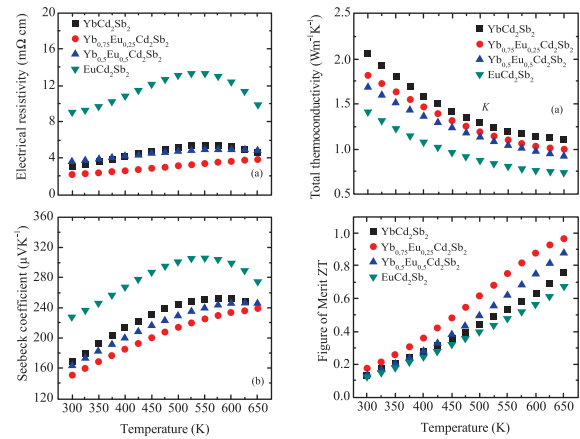


Fig. 3: High temperature thermoelectric properties of the  $\text{Yb}_x\text{Eu}_{1-x}\text{Cd}_2\text{Sb}_2$  compounds.

In summary, three compositions with  $ZT > 1$  were obtained. Among them  $\text{YbCd}_{1.6}\text{Zn}_{0.4}\text{Sb}_2$  exhibits the highest  $ZT$  value we achieved so far, with a maximum value of 1.2 at 700 K. Our investigations also demonstrate the potential of the Zintl phases for thermoelectric applications. Further optimization of the thermoelectric properties of these compounds might be realized through partial substitutions on the three crystallographic sites of the crystal structure.

### $\text{Ru}_{1-y}\text{In}_3$

The phase  $\text{Ru}_{1-y}\text{In}_3$  belongs to the  $TME_3$  family of compounds, where  $TM$  is a transition metal from group 8 or 9 and  $E$  is a metal of group 13, respectively. These phases differ in their valence electron concentration (VEC): 17-electron compounds exhibit semiconducting behavior while 18-electron compounds are metals [11]. Ruthenium and indium represent the heaviest known low-toxic combination of elements that composes a 17-electron configuration. For this reason we have focused our investigations to the potential of  $\text{Ru}_{1-y}\text{In}_3$  and its substitution variants  $\text{RuIn}_{3-x}\text{A}_x$  ( $A = \text{Sn}, \text{Zn}$ ) as new TE materials [12].

The crystal structure of  $\text{Ru}_{1-y}\text{In}_3$  belongs to the  $\text{FeGa}_3$  type (space group  $P4_2/mnm$ , no. 136) and can be described as a 3D packing of polyhedra. The main building unit is a trigonal prism, composed of In atoms centred by Ru; two additional In atoms cap the two square faces of the prism. Two of these

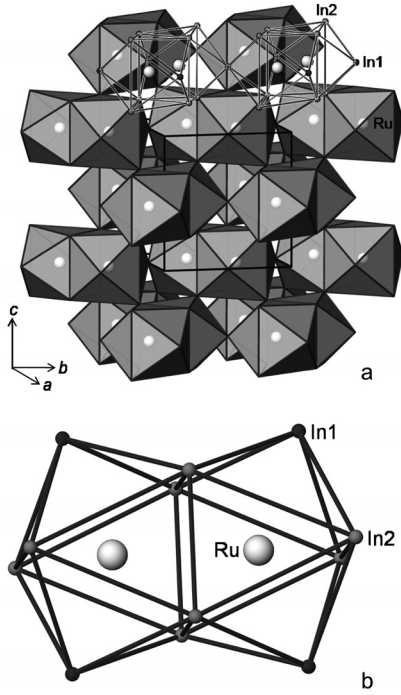


Fig. 4: Polyhedral representation of the crystal structure of  $\text{RuIn}_3$  (a) and its trigonal prisms of building units with shared faces and double caps  $[\text{Ru}_2(\text{In1})_2(\text{In2})_4]$  (b).

bi-capped trigonal prisms share a common face, such that each Ru is simultaneously at the center of a prism and caps the adjacent one. In the unit cell these building units are interlinked by sharing In2 corners in the  $[001]$  direction and via common In1 atoms in the  $(001)$  plane. This way, a three-dimensional network is formed.

From the X-ray diffraction patterns of  $\text{Ru}_{1-y}\text{In}_3$  samples, the lattice parameter  $a$  practically does not change with Ru content, while the value of  $c$  increases for the more In-rich samples and decreases in the In-poor ones. This indicates the existence of a homogeneity range in  $\text{Ru}_{1-y}\text{In}_3$  caused most probably by the defect occupation of the Ru site. Substitution of In by Zn or Sn leads in both cases to a reduction of the lattice parameter  $c$ , again leaving  $a$  unchanged. This behavior may be explained by the preferential occupation of the In1 position with Sn or Zn at small substitution ratios.

The calculated electronic density of states (DOS) for  $\text{RuIn}_3$  (Fig. 5) shows a band gap of  $\sim 0.3$  eV that is slightly smaller than the experimental observation of  $\sim 0.45$  eV. The DOS of  $\text{RuIn}_{3-x}\text{Sn}_x$  for a series of Sn concentrations (virtual crystal approximation) reveals an almost rigid-band-like behavior for small Sn concentrations, especially in

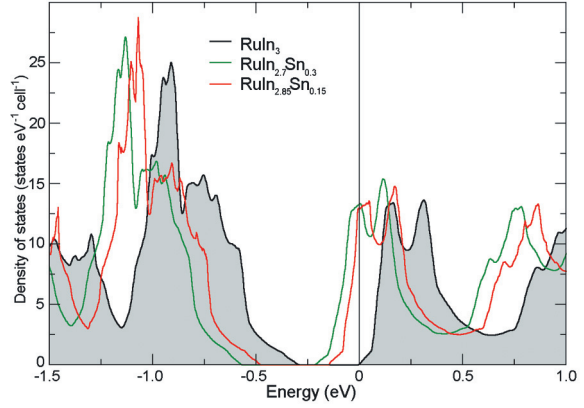


Fig. 5: Calculated total electronic density of states for  $\text{RuIn}_3$  and the substitution-derivatives  $\text{RuIn}_{3-x}\text{Sn}_x$  ( $x = 0.15$  and  $0.30$ ) close to the Fermi level. The latter is indicated by the vertical line.

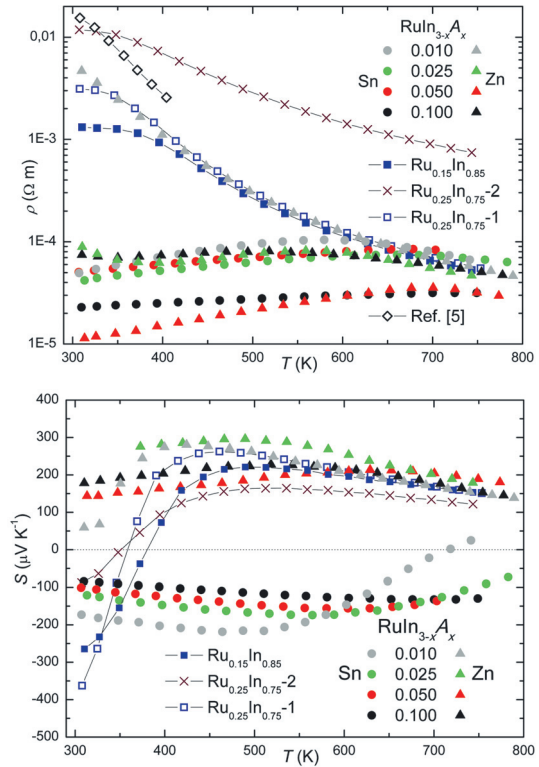


Fig. 6: Temperature dependence of the electrical resistivity (upper panel) and thermopower (lower panel) of  $\text{Ru}_{1-y}\text{In}_3$ ,  $\text{RuIn}_{3-x}\text{Sn}_x$  and  $\text{RuIn}_{3-x}\text{Zn}_x$ .

the relevant region close to the Fermi level. This is in qualitative agreement with the experimentally obtained thermopower values, which decrease upon an increased substitution of In by Sn or Zn.

The binary  $\text{Ru}_{1-y}\text{In}_3$  samples exhibit a semiconducting behavior (Fig. 6). After a short plateau, the resistivity decreases significantly above 350 K by

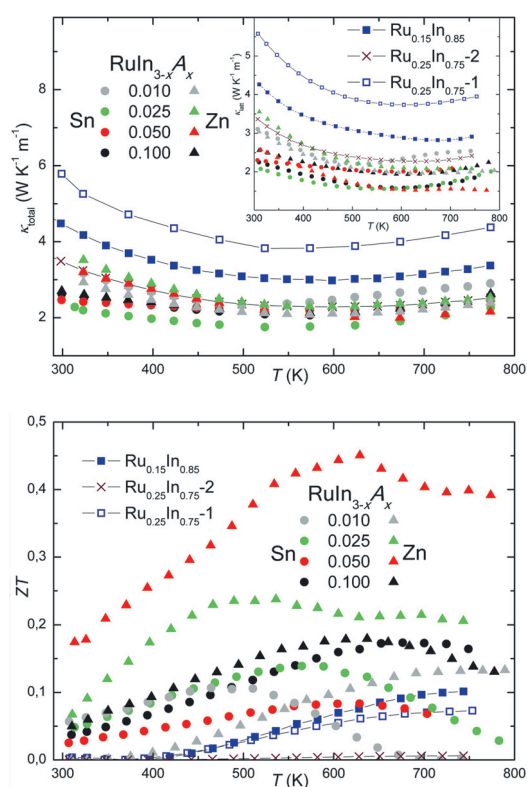


Fig. 7: Temperature dependence of the thermal conductivity (upper panel) and  $ZT$  (lower panel) of  $\text{Ru}_{1-y}\text{In}_3$ ,  $\text{RuIn}_{3-x}\text{Sn}_x$  and  $\text{RuIn}_{3-x}\text{Zn}_x$ .

more than one order of magnitude. The experimental band gap of 0.45 eV is in good agreement with the values of 0.4 and 0.5 eV obtained experimentally for the  $\text{RuIn}_3$  single crystal along different crystallographic directions [13]. In accordance with the electronic density of states, the electrical resistivity decreases with increasing  $y$ . In contrast to the semiconducting properties of binary  $\text{Ru}_{1-y}\text{In}_3$ , all substitution variants feature metal-like behavior, indicated by a constantly increasing resistivity with increasing temperatures. All  $\text{RuIn}_{3-x}\text{Sn}_x$  and  $\text{RuIn}_{3-x}\text{Zn}_x$  compounds exhibit a local maximum of resistivity implying activated behavior of a heavily doped semiconductor, which does depend on the doping level but not on the doping species. Furthermore, an increase in  $x$  results in an increase in the carrier concentration thereby giving rise to a lower electrical resistivity. The thermal conductivity of  $\text{RuIn}_{3-x}\text{Sn}_x$  and  $\text{RuIn}_{3-x}\text{Zn}_x$  depends only slightly on temperature, with a shallow minimum between 500 K and 600 K (Figure 7). In general, all substituted materials show a similar reduction of the thermal conductivity of nearly 50% with

respect to that of  $\text{RuIn}_3$ . The small increase of the thermal conductivity of all materials at temperatures above 600 K most likely arises from the thermal excitation of minority carriers across the band gap. The electronic contribution  $\kappa_{\text{el}}$ , which can be derived from the Wiedemann-Franz law  $\kappa_{\text{el}} = LT/\rho$ , where  $L$  is the Lorenz number of  $2.4510^{-8} \text{ V}^2 \text{ K}^{-2}$ , increases with increasing temperature. Because of the low values of  $\kappa_{\text{el}}$  the thermal conductivity is mainly determined by the lattice contribution.

The dimensionless figure of merit for  $\text{Ru}_{1-y}\text{In}_3$  and its derivatives is plotted in Figure 7 as a function of temperature. While the binary  $\text{Ru}_{1-y}\text{In}_3$  exhibits a rather low  $ZT$  of 0.07 at 753 K, this value increases upon substitution up to 0.17 at 676 K for the highest tin-substituted composition  $\text{RuIn}_{2.90}\text{Sn}_{0.10}$ . However, substituting  $\text{Ru}_{1-y}\text{In}_3$  with Zn is a more effective way to improve the  $ZT$  value reaching 0.45 at 630 K for  $\text{RuIn}_{2.95}\text{Zn}_{0.05}$ . This value is nearly three times higher than the values obtained with Sn and indicates that significant improvements of the thermoelectric properties in the class of  $\text{TME}_3$  compounds can be achieved via partial substitutions.

## References

- [1] (a) G. J. Snyder and E. S. Toberer, *Nature Mater.* **7** (2008) 105. (b) S. Paschen, C. Godart and Yu. Grin in *Complex Metallic Alloys: Fundamentals and Applications*. (Wiley-VCH) (2011) 365.
- [2] D. M. Rowe in *CRC Handbook of Thermoelectrics* (1995).
- [3] H. Zhang *et al.*, *Intermetallics* **18** (2010) 193.
- [4] H. Zhang *et al.*, *J. Chem. Phys.* **129** (2008) 164713.
- [5] H. Zhang *et al.*, *Dalton Trans.* **39** (2010) 1101.
- [6] H. Zhang *et al.*, *Intermetallics* **18** (2010) 193.
- [7] H. Zhang *et al.*, *J. Elec. Mater.* **39** (2010) 1772.
- [8] Q.-G. Cao *et al.*, *J. Appl. Phys.* **107** (2010) 053714.
- [9] X.-J. Wang *et al.*, *Appl. Phys. Lett.* **94** (2009) 092106.
- [10] H. Zhang *et al.*, *J. Chem. Phys.* **133** (2010) 194701.
- [11] U. Häussermann *et al.*, *J. Sol. Stat. Chem.* **165** (2002) 94.
- [12] M. Wagner *et al.*, *J. Mat. Res.* **26** (2011) 1886.
- [13] D. Bogolanov *et al.*, *J. Phys.: Condens. Matter* **19** (2007) 232202.

<sup>1</sup> Present address: MPG-CAS Partner Group, Key Laboratory of Transparent Opto-Functional Inorganic Materials of Chinese Academy of Sciences (Shanghai Institute of Ceramics), 1295 Dingxi road, 200050 Shanghai, China